Original Research

Journal of Advanced Veterinary Research
(2024) Volume 14, Issue 5, 831-837

Furan and cadmium combined treatment-potentiated renal damage: Role of oxidative damage

Shrouk Amer[1], Ragab Elshawarby[1], Nabila M. Abdelaleem[1], Elham Elshewy[1], Afaf Abdelkader[2], Ahmed B. Zaid[3], Ahmed Abdeen[1*]

[1]*Department of Forensic Medicine and Toxicology, Faculty of Veterinary Medicine, Benha University, Toukh 13736, Egypt.*
[2]*Department of Forensic Medicine and Clinical Toxicology, Faculty of Medicine, Benha University, Benha 13518, Egypt.*
[3]*Department of Clinical Pathology, National Liver Institute, Menoufia University, Shibin Elkom 32511, Egypt.*

ARTICLE INFO

Recieved: 04 January 2024

Accepted: 17 February 2024

***Correspondence:**

Corresponding author: Ahmed Abdeen
E-mail address: ahmed.abdeen@fvtm.bu.edu.eg

Keywords:

Nephrotoxicity
Aquaporins
Combined toxicity
Kim-1
Apoptosis
Inflammatory markers
INOS

ABSTRACT

Furan (FU) is a common food contaminant and environmental pollutant. While cadmium (Cd) is a prevalent environmental contaminant that poses a risk to the health of humans and animals. The goal of the current study was to assess the combined effects of FU and Cd on the kidney of male albino rats. Five groups of rats were designed: Cr-water, Cr-oil, FU (16 mg/kg b.w), Cd (2 mg/kg b.w), and FU+Cd, rats were co-treated with both FU and Cd. All treatments were given orally for 30 days. Renal function testing revealed severe biochemical changes in the rats, indicating substantial tissue injury. In addition, there was a notable rise in malondialdehyde (MDA) levels and a fall in reduced glutathione (GSH) concentration as well as the activity of superoxide dismutase (SOD) and catalase (CAT). Also, prominent histopathological alterations in renal tissues were noticed. Additionally, FU and/or Cd significantly up-regulated the expression profile of Kim-1, and inflammatory markers (TNF-α and iNOS). Meanwhile, Aqp1, and Aqp2 m-RNA genes expression were significantly downregulated along with significant upregulation of apoptotic proteins (PCNA). Intriguingly, the concurrent FU and Cd intoxication elicited additional extensive renal injury than their individual exposure.

Introduction

In recent years, it has been discovered that improper food processing affects the structure and integrity of bio-organic molecules found in food, including carbohydrates, proteins, lipids, and nucleic acids, resulting in the formation of unpleasant chemicals like furan (FU) (Starowicz *et al*., 2021). FU (C4H4O), is a colorless, naturally occurring extremely volatile liquid, and heterocyclic carcinogenic molecule. The National Toxicology Program and the International Agency for Research on Cancer have classified it as a probable human carcinogen (Group 2B) (Batool *et al*., 2021). FU is a prominent industrial product that is mostly used as an intermediary in the synthesis of various solvents, lacquers, resins, and chemical and pharmacological substances (Seok *et al*., 2015). It frequently occurs in a number of thermally driven meals, including various coffees, infant foods, cereals, and meat products (Batool *et al*., 2021). It has drawn attention from all around the world due to its wide dispersion throughout the ecosystem, including the air, soil, and water (Seok *et al*., 2015). Cytochrome P450 2E1 is implicated in the conversion of FU to the hazardous reactive intermediate, cis-but-ene-1,4-dialdehyde (BDA), which react with amino acids, proteins, and nucleic acid sequences to cause toxicities in significant bodily organs (Owumi *et al*., 2022a).

Furthermore, contamination of food and feedstuffs with heavy metals poses risks to human and animal health, and as a result, is a topic of interest globally (Seif *et al*., 2019). Among heavy metals, Cd is one of 126 priority pollutants because of the numerous health risks it poses to all types of creatures found in the Earth's biosphere. Based on substantial evidence of carcinogenesis in human and animal research, the International Agency for Research on Cancer designated Cd as a human carcinogen (group 1) (IARC, 2012). Cd is widely used in plastics, battery, metal plating, pigment, fertilizer, and different alloy sectors contributes in its availability in the environment (air, water, and soil) (Kumar and Sharma, 2018). Cd mostly enters the bodies of organisms through the skin, digestive system, and respiratory system (Setia *et al*., 2020). Due to its physicochemical properties, an excess of this element in the body can harm the liver, kidneys, testes, and lung as well as result in a number of complications like apoptosis, anemia, genotoxicity , hepatic damage, bone, and renal illnesses (Filipič, 2012; Brzóska *et al*., 2015). It is possible for Cd to cause inflammation, lipid peroxidation, depletion of glutathione (GSH), reactive oxygen species (ROS), and protein cross-linking when it is released into the cytoplasm. Consequently, kidney injury is caused by the accumulation of proinflammatory cytokines and the death of renal cells (Ansari *et al*., 2017). It is generally known that Cd has a strong affinity for many biological elements, particularly cellular molecules that contain the sulfur compound sulfhydryl (SH), particularly metallothionein (MT). According to Rani *et al*. (2014), MT is known to be essential for the detoxification of Cd. Hepatocytes form the Cd-MT complex, which is then transported to the kidney and causes nephrotoxicity (Klaassen *et al*., 2009).

Kidney damage from toxic load is well known to occur because of increased perfusion and larger concentrations of discharged toxins throughout the renal tubules. Based on the above-mentioned, in many circumstances, FU and Cd can be consumed by humans and farm animals where there are no rigorous regulations against heavy metal contamination and the level of thermal processing of foods which prone individuals to both systemic and local toxicity. Cd toxicity is well studied, and FU has earned a position on the IARC's list of carcinogens. Thus, the current study was setup to assess the detrimental effects of FU and/or Cd exposure on renal tissue in a rat model by measuring kidney function tests, oxidative/antioxidative status, histopathological changes, immunohisto-

ISSN: 2090-6277/2090-6269/

chemical alterations, and genes expression of inflammatory markers and Aquaporins (AQPs).

Materials and methods

Chemicals

FU (CAS No. 109-99-9; 99.5% Extra pure; LOBA CHEMIE PVT.LTD.) Jehangir Villa, 107 Wode House Road, Mumbai, Maharashtra 400005, India. The source of the Cd was Central Drug House Ltd. in New Delhi, India.

Animals and experimental design

A total of 50 adult male Wister Albino rats weighing between 160-200 g were used in the current investigation. Rats were provided by the Centre of Laboratory Animals at the Faculty of Veterinary Medicine, Benha University in Egypt. After that, they were housed in a well-ventilated area, (25.0±3.0°C temperature, and 45-55 % relative humidity) with free access to water and a normal pellet diet. This experiment was endorsed by the Institutional Animal Care and Use Research Ethical Committee of the Faculty of Veterinary Medicine, Benha University (BUFVTM 01–05- 23).

After two weeks of acclimatization, rats were haphazardly allocated into five groups, (Each with 10 rats). Control groups: Cr-water (rats were given water as a vehicle for Cd) and Cr-oil (rats received corn oil as a vehicle for FU). FU group, in which rats were administered FU (16 mg/kg b.w) (McDaniel *et al*., 2012). Cd group, in which rats received $CdCL_2$ (2 mg/kg b.w) (Abdeen *et al*., 2019a). FU+Cd group, rats were co-treated with both FU and Cd at the same above-mentioned dosages for 30 consecutive days. All treatments were administered daily by gavage tube.

Samples collection and processing

At the end of the experiment, rats were fasted overnight, and blood samples were collected from the hepatic vein of each rat after was euthanized under isoflurane inhalation anesthesia. The sera were isolated after centrifugation at 4000 rpm for 10 min using cooling centrifuge (DLAB D3024R High Speed Micro-Centrifuge, USA) and maintained at -20°C for biochemical assays.

The kidney tissues were removed quickly, and any potential blood congealment and RBCs were removed by washing them in both normal saline solution and sodium phosphate buffered saline. Then the tissue was divided into sections for further tissue processing (evaluation of oxidative indicators, histopathological, immunohistochemistry, and gene expression). The section used for gene expression quickly frozen in liquid nitrogen and kept at -80 °C for total RNA extraction and subsequent molecular investigation of genes expression.

Biochemical assay

Serum urea, creatinine, uric acid, total protein, and albumin were measured by chemical kits that were purchased from Bio-diagnostics Co., Cairo, Egypt. All procedures were followed in compliance with the guidelines provided by the manufacturer.

Tissue oxidative biomarkers assay

One gram of renal tissue was homogenized using a sonic homogenizer in 5 ml of cold buffer solution (50 mmol K_3PO_4, 1 mmol EDTA, pH 7.5). Following that, the homogenate was centrifuged at 4000 rpm for 20 min in a cooled centrifuge. The supernatant was collected and used for measures of malondialdehyde (MDA), glutathione (GSH), Superoxide dismutase (SOD) content, and activity of Catalase (CAT), Bio-diagnostic Company (Giza, Egypt).

Assessment of Kim-1, iNOS, Aqp1, and Aqp2 Gene Expression

Trizol reagent was used to isolate total RNA from kidney samples in compliance with the manufacturer's instructions (Direct-zolTM RNA MiniPrep, catalogue No. R2050). Utilizing a Nanodrop (UV-Vis spectrophotometer Q5000/USA), the amount and purity were determined, and gel electrophoresis was used to assess the integrity. After that, the RNA samples were reverse-transcribed into cDNA in accordance with the manufacturer's instructions (SensiFastTM cDNA synthesis kit, Bioline, catlog No. Bio- 65053). Twenty microliters were the entire volume of the reaction mixture, which included one microliter of reverse transcriptase, one microliter of total RNA up to one microgram, four microliters of 5x Trans Amp buffer, and twenty microliters of DNase-free water. The final reaction mixture was put in a thermal cycler, and the following protocol was run; primer annealing for 10 min at 25°C, reverse transcription for 15 min at 42°C, and inactivation for 5 min at 85°C. The samples were stored at 4°C.

Real-time PCR utilizing SYBR Green PCR Master Mix (2x SensiFastTM SYBR, Bioline, catlog No. Bio-98002) was used to assess the relative renal mRNA abundance of Kim-1, iNOS, Aqp1, and Aqp2. The primer sequence used for qRT-PCR analysis is shown in Table 1. Internal control was provided by the housekeeping gene β-Actin. A total of 20 µL was used for the reaction mixture, which included 10 µL of 2x SensiFast SYBR, 3 µL of cDNA, 5.4 µl of H_2O (d.d. water), and 0.8 µl of each primer. The following parameters were used for the real-time PCR: 95°C for 4 min, 40 cycles of 94°C for 15 sec, annealing temperatures of 58°C for 30 sec, and extension temperatures of 72°C for 20 sec. A melting curve analysis was carried out to verify the PCR product's specificity at the final stage of the amplification phase. In order to standardize the levels of target gene expression, the $2^{-\Delta\Delta Ct}$ technique was utilized to quantify the relative expression of each gene in each sample relative to β-Actin gene as a control (Pfaffl, 2001).

Histoarchitecture inspection

Slices of fresh kidney tissues were fixed in 10% neutral buffered formalin, dried in ethanol at varying concentrations, cleared in xylene,

Table 1. Listing of the used primers for real-time PCR amplifications.

Genes	GenBank accession number	Oligonucleotide sequence	Size (bp)
Kim-1	AF035963.1	f5,- AGACAGAGTGTGCTGAGTGC-3, r5, -ACAGAGCCTGGAAGAAGCAG-3,	121
Aqp1	NM_012778.2	f5,- GTGACTCCAGGCACAGTCTC-3, r5, -ATGGTTAACGGCACAGTGGT-3,	168
Aqp2	NM_012909.3	f5,- GAGAGACGGAGAGCTCTGG-3, r5, - TGTATCACCACAGGCACTCG-3,	190
iNOS	NM_012611.3	f5,- TGGGTGAAAGCGGTGTTCTT -3, r5,- TAGCGCTTCCGACTTCCTTG -3,	108
β-Actin	NM_031144.3	f5,- GGCATGTGCAAGGCCGGCTT -3, r5,- TAGGAGTCCTTCTGACCCATA -3,	116

and embedded in paraffin. Sections of (4-6 µm) thickness were cut from the paraffin blocks and stained with hematoxylin and eosin (H&E) for screening and images, using a camera integrated digital imaging system (CH9435 Hee56rbrugg) (Leica Microsystems, Switzerland).

Immunohistochemical assessment

The avidin-biotin-peroxidase complex (ABC) technique was used to apply immunohistochemistry to paraffinized tissue slices that had been fixed on positively charged slides. Both mouse anti-TNF alpha monoclonal antibody (Elabscience Cat# E-AB-22159, Dilution: 1:50) and rabbit anti-PCNA polyclonal antibody (Elabscience Cat# E-AB-64562, Dilution: 1:50) have undergone testing. Sections from each study groups were pre-incubated with the aforementioned antibodies before being treated with the reagents needed for the ABC method (Vectastain ABC-HRP kit, Vector labs). In order to differentiate between antigen-antibody complexes, markers were expressed, recognized using peroxidase, and stained with diaminobenzidine (DAB, made by Sigma). Instead of employing primary or secondary antibodies, negative controls were implemented using non-immune serum. Using a Leica microscope (CH9435 Hee56rbrugg) (Leica Microsystems, Switzerland), immuno-stained slices were examined and captured on camera at various magnification levels.

For quantitative scoring of immunohistochemical results, analysis of each serial sections of the investigated groups, six high power fields (x 400) with positive brown immunostaining were chosen. The Leica QWin 500 image analyzer computer system (England) was used to calculate the area% for sections stained with PCNA, and TNF alpha. This image analyzer includes a Leica microscope, a colored camera, a colored display, and a hard drive of an IBM Leica personal computer connected to the microscope and controlled by Leica QWin 500 software. Statistics were used to explain the data for each antibody in terms of mean and standard deviation (mean ± SD) for area%.

Data analysis

The statistical tests were carried out using SPSS software (version 21.0; SPSS Inc., Chicago, IL, United States). The various data sets were compared using One-way ANOVA and Duncan's post hoc test. A mean ± SD is displayed for the results. When $p \leq 0.05$, values were deemed statistically significant.

Results

Biochemical assay

As shown in Figure 1, FU, Cd, and FU+Cd groups treatment resulted in renal injury, which was demonstrated by abnormally high level of various markers, such as urea, creatinine, and uric acid in serum. Additionally, there was a discernible drop in total protein and albumin levels compared to control group. Remarkably, when rats were co-exposed to both agents, more notable renal dysfunctions were observed than their individual exposure.

Kidney oxidative/antioxidative markers

Figure 2 displays the antioxidant enzymes data, in response to FU and/or Cd exposure, renal tissues showed a substantial decrease in GSH, SOD, and CAT activities and a sharp rise in MDA levels relative to control. Interestingly, exposure to both toxins could evidently cause greater oxidative damage in the kidneys than exposure to either toxin solo.

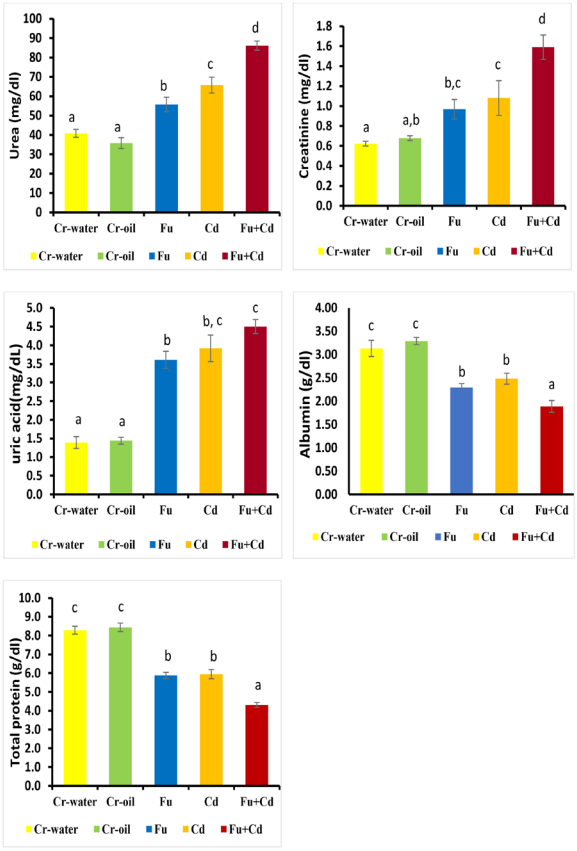

Fig. 1. Changes in serum biochemical parameters of rat after treatment with FU and/or Cd. All values are expressed as the mean ± SE (n = 6). Superscript letters within the same rows were significant ($p \leq 0.05$). FU, Furan; Cd, Cadmium.

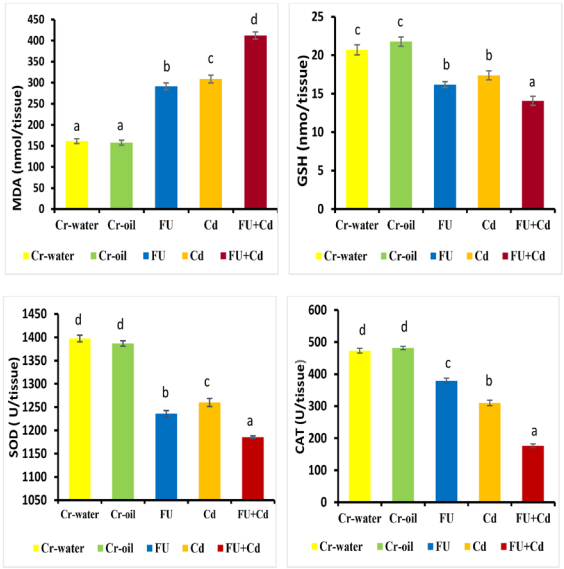

Fig. 2. Changes in oxidative/antioxidative status in kidney tissues of rat after treatment with FU and/or Cd. All values are expressed as the mean ± SE (n = 5). Superscript letters within the same rows were significant ($p \leq 0.05$). MDA, malondialdehyde; GSH, glutathione; SOD, superoxide dismutase; CAT, catalase; FU, Furan; Cd, Cadmium

Assessment of Kim-1, Aqp1, and Aqp2 gene expression

mRNA expression of Kim-1, Aqp1, and Aqp2 were investigated in the renal tissue (Figure 3). Overall FU and/or Cd treated rats could modulate gene expression compared to control group. There was marked up-regulation in the expression profile of Kim-1. While Aqp1 and Aqp2 were significantly downregulated. Remarkably, there was severe modulation in gene expression in the kidney tissue when rats were exposed to both agents than their individual.

Renal expression of proinflammatory cytokine

As seen in Figure 3, exposure to FU or Cd triggered an inflammatory response in the kidney tissue as evidenced by a marked up-regulation of the levels of the mRNAs for iNOS in confront to controls. Remarkably, when FU was administrated concurrently with Cd, kidney samples exhibited more inflammatory damaging effects indicated by increased expression of iNOS than their individual treatments.

Also, immunohistochemical expression of TNFα in kidney tissues are depicted in Figure 5, FU or Cd intoxication induced significant moderate positive cytoplasmic expression of TNF-α in glomerulus and renal tubules in confront to few positive cytoplasmic expressions in the control tissues. interestingly, combined treatment with FU and Cd revealed intense positive cytoplasmic expression of TNFα when compared to their sole exposure.

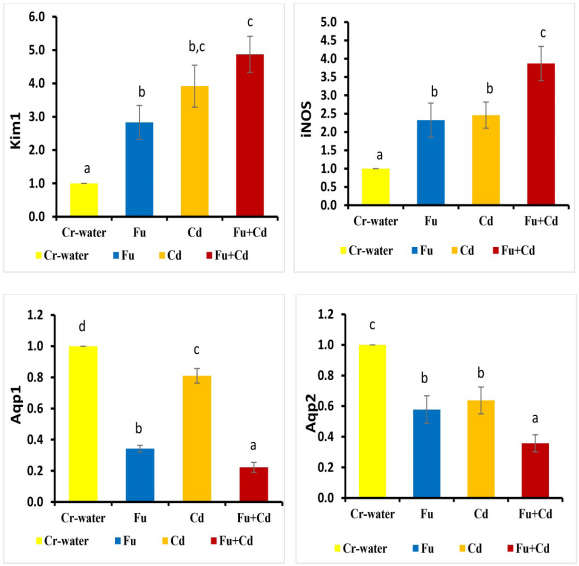

Fig. 3. Relative expression of Kim-1, iNOS, Aqp1, and Aqp2 in in kidney tissues after treatment with FU and/or Cd. All values are expressed as the mean ± SE (n = 4). Superscript letters within the same rows were significant ($p \leq 0.05$). FU, Furan; Cd, Cadmium.

Histoarchitecture examination

The renal histological changes were evaluated in order to provide further validation for the previously mentioned results subsequent to FU and/or Cd exposure (Figure 4). Cr-water group (a) and Cr-oil group (b) showed the normal architectures of renal cortex (normal glomerulus, bowmen's capsule, PCT, and DCT). Contrary to the control, the FU-group (c) showed degeneration of renal cortex, and vacuolation of glomeruli. Renal tubules existed with karyolitic changes, interstitial hemorrhage, hyalinization, epithelial desquamation, inflammatory cells infiltration, and others suffered from necrotic changes. Interestingly, when FU was co-administrated with Cd (e), the kidney tissue revealed severe injury of renal cortex and degeneration of renal corpuscle with vacuolation of glomeruli. Renal tubules lose their normal organization and lined with deep basophilic apoptotic nuclei, some tubules appear with hyalinization, necrosis, and dilatation. Additionally, some tubules presented with epithelial desquamation and Interstitial hemorrhage. Scoring of histological alteration induced by FU and/or Cd in the kidney is done in Table 2.

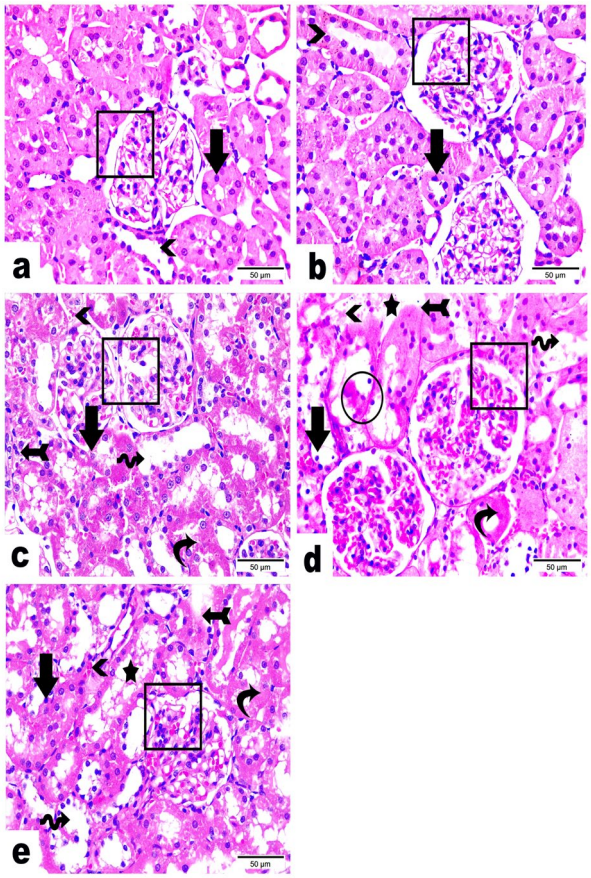

Fig. 4. Kidney histoarchitecture after treatment with FU and/or Cd. Cr-water group (a) Cr-oil group (b) showed the normal architecture of renal cortex (normal glomerulus, bowmen's capsule (rectangles), PCT (arrows), and DCT (arrowheads)). FU group (c) showed moderate degenerative changes in the kidney tissue with capsule hyalinization and vacuolation of glomerulus (rectangle). Some renal tubules show karyolitic changes (arrow), dilatation (wave arrow), necrotic areas (curvy arrow), interstitial hemorrhage (arrowhead), and inflammatory cells infiltration (arrow with tail). Cd group (d) displayed some degeneration in renal cortex with hypertrophy of renal corpuscle and degeneration of bowmen's capsule (rectangle). Some renal tubules showed detached endothelial lining and surrounded with deep basophilic apoptotic cells (arrow), epithelial desquamation (circle), hyalinization (arrow with tail), dilated tubule (wave arrow), necrotic changes (curvy arrow), additionally interstitial hemorrhage (arrowhead), interstitial edema leading to dispersion between renal tubules (star). FU+Cd group (e) revealed severe injury along renal cortex area noticed in degeneration of renal corpuscle with vacuolation of glomerulus (rectangle). Disorganized renal tubules lined with deep basophilic apoptotic nuclei (arrow), with hyalinization of some tubules (arrow with tail), necrosis (curvy arrow), dilated tubule (wave arrow), were also present. Additionally, some tubules showed epithelial desquamation (star), and interstitial hemorrhage (arrowhead). H&E-stained sections (Bars = 50 µm).

Evaluation of apoptosis in renal tissues

Changes in PCNA immunohistology expressions in nuclei of kidney tissues are illustrated in Figure 6. FU (c) or Cd (d) exposure exhibited significant moderate positive nuclear expression of PCNA in glomeruli and renal tubules in comparison to few positive nuclear expressions in the control tissues. Notably, synchronous exposure to both remedies revealed intense positive nuclear expression of PCNA.

Table 2. Ordinal scoring of histological alteration induced by FU and/or Cd in kidney.

Parameters	Experimental groups				
	Control water	Control corn oil	FU	Cd	FU + Cd
Number of degenerated Tubules	2.50± 0.43^{a}	2.17± 0.48^{a}	21.00± 1.53^{b}	21.50± 1.34^{b}	33.00± 1.06^{c}
Area of Interstitial Hemorrhage	0.39± 0.14^{a}	0.30± 0.04^{a}	14.80± 1.01^{b}	15.12 ±1.33^{b}	23.46± 0.96^{c}
Area of Interstitial Edema	1.95± 0.38^{a}	2.04± 0.34^{a}	7.65± 0.64^{b}	7.55 ±1.10^{b}	15.44± 1.40^{c}

All values are expressed as the mean ± SE. Superscript letters within the same rows were significant ($p \leq 0.05$). FU, Furan; Cd, Cadmium.

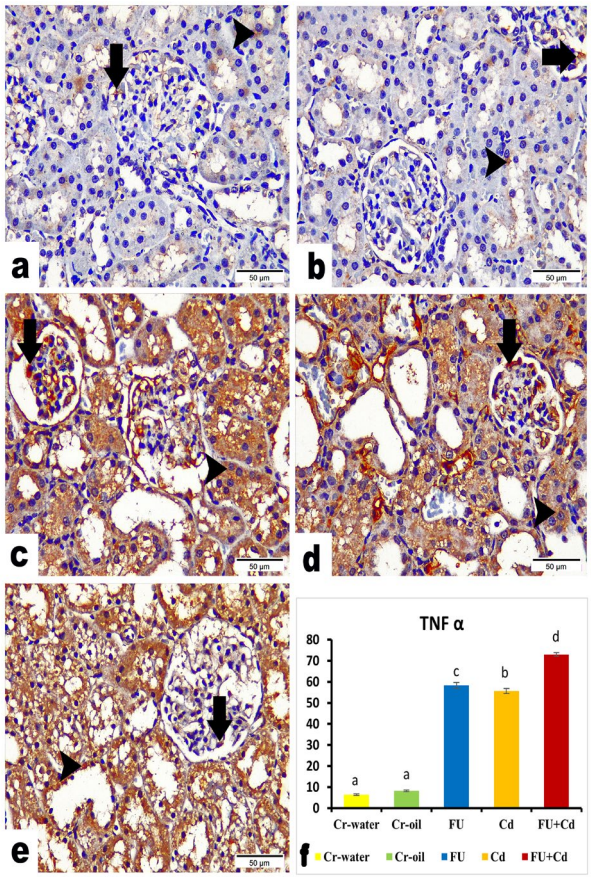

Fig. 5. Effects of FU and/or Cd on the expression of TNFα in the kidney tissue. Cr-water (a) and Cr-oil (b) groups showed few positive cytoplasmic expressions of TNF-α in the glomeruli and renal tubules. FU or Cd-treated rats exhibited moderate positive cytoplasmic expression of TNF-α (c and d, respectively). While FU+Cd (e) treated rats displayed intense positive cytoplasmic expression of TNF-α. P< 0.05. Values were expressed as mean ± SE. The column chart shows the scoring of TNF-α expression in kidney tissue among different treated groups (f). FU, Furan; Cd, cadmium; arrow, Glomeruli; arrowhead, renal tubules. (Scale bar = 50 µm).

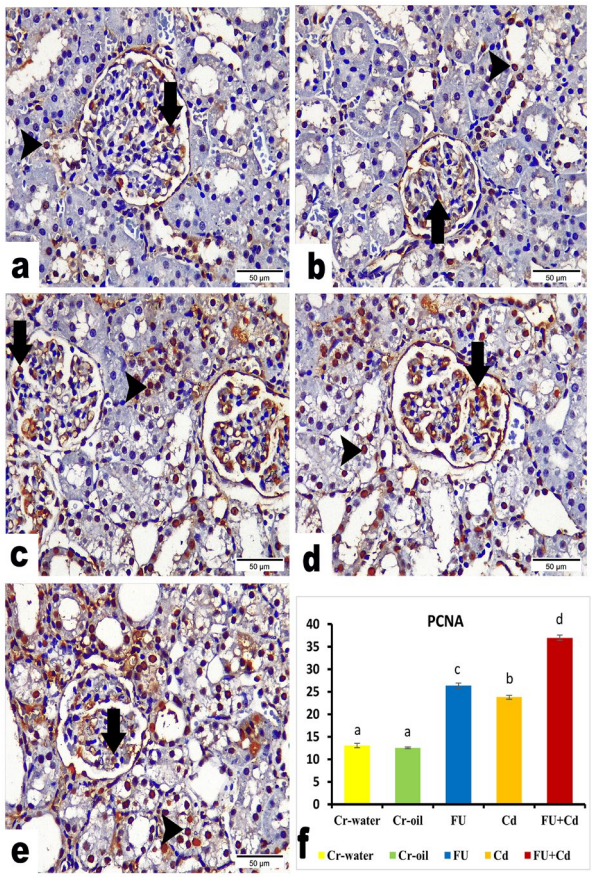

Fig. 6. Effects of FU and/or Cd on the expression of PCNA in the kidney tissue. Cr-water (a) and Cr-oil (b) groups showed very few positive nuclear expressions of PCNA in the glomeruli and renal tubules. FU or Cd -treated rats exhibited moderate positive nuclear expression of PCNA (c and d, respectively). While FU+Cd (e) treated rats displayed intense positive nuclear expression of PCNA. P< 0.05. Values were expressed as mean ± SE. The column chart shows the scoring of PCNA expression in kidney tissue among different treated groups (f) FU, FU, Furan; Cd, cadmium; arrow, Glomeruli; arrowhead, renal tubules. (Scale bar = 50 µm).

Discussion

FU is produced as a byproduct of the thermal processing of food and has harmful effects on the health of organisms. Additionally, it is found in the environment since it is a significant component of smoke from cigarettes, wood, and exhaust from motor engines (Tăbăran *et al*., 2019). Therefore, it is consumed by humans through food and air, stored in mammalian fat tissues over time and can enter into the blood under stress or hunger (Yilmaz, *et al*., 2017) . Moreover, Cd is a non-essential heavy metal that is extremely toxic and has adverse effects on the majority of human and animal organ systems, leading to multisystem illness. It is regarded as a possible global environmental danger (Rahimzadeh *et al*., 2017).

According to Dong *et al*. (2016), oxido-inflammatory reactions and cellular proliferation are the mechanisms associated with FU toxicity. Upon oral exposure, the oxidation of the FU ring is catalyzed by cytochrome P450 producing reactive BDA. This toxic metabolite can then irreversibly bind to DNA, lipid, and protein, causing the most harmful effects of FU on different body system (Phillips *et al*., 2014). Moreover, The build-up of Cd in tissues, especially in the liver and kidneys, results in early oxidative stress and a variety of pathological disorders (Cabral *et al*., 2021). Cd bind to sulfhydryl (-SH) groups of proteins that scavenge ROS and non-protein molecules like GSH, oxidative stress and ROS are indirectly increased, as shown by lipid peroxidation and cell death (Olayan *et al*., 2020). Along with GSH depletion, Cd may bond with the protein structure of the enzyme, creating an impairment of its catalytic activity, and substitute the other divalent cation required for the activity of antioxidant enzymes (Almeer *et al*., 2018).

The prevalent toxic pathways attributed to tissue damage caused by FU and Cd include oxidative stress, inflammatory responses, and mitochondrial dysfunction (Owumi *et al*., 2022b; Poli *et al*., 2022). According to Abdeen *et al*. (2019a), oxidative distress is well known for starting when generated ROS, such as hydroxyl radicals ($HO^{\bullet}$), hydrogen peroxide (H_2O_2), superoxide anions ($O_2^{\bullet-}$), surpass the body's natural antioxidant capacity. Lipid peroxidation, decreased ATP synthesis, protein misfolding, and DNA damage are the main hallmarks of oxidative stress in biological systems (Uddin *et al*., 2021).

The current research reveals compelling evidence that ROS were a contributor in the harmful effects of FU and/or Cd treatment, which indicated by marked depletion in GSH, a non-enzymatic antioxidant, SOD, and CAT, an enzyme-based antioxidant, along with prominent increase in MDA content in the renal tissue. However, compared to other groups, there has been more notable renal oxidative damage when both medications are used together. These antioxidant enzymes safeguard cellular constituents from the damage of free radicals. CAT safeguards the cell from oxidative damage triggered by oxygen species since it is essential for breaking down H_2O_2 into H_2O and O_2. Therefore, in a situation where the overproduction of ROS caused by FU and/or Cd depletes CAT activity, large volumes of $OH^{\bullet}$ are produced by Fenton's reaction from H_2O_2, which instantly assaults the membrane lipid and raises the production of MDA and LPO. In addition to CAT, GSH is another endogenous antioxidant that is plentiful in all biological systems having ability to actively scavenge ROS (Abdel-Daim *et al*., 2021). It is believed that FU argument GSH deficiency, which damages the antioxidant defense mechanism of the cell and creates the circumstances for free radicals to harm cells (Alizadeh *et al*., 2018). Moreover, in renal epithelial cells, Cd merely combines with the SH content of GSH to create the GSH-Cd complex, which is less easily reabsorbed than the Cd-MT complex (Samarghandian *et al*., 2015). Our result aligns with previous research of Owumi *et al*. (2022a) and Ijaz *et al*. (2023) suggesting that decreased GSH levels in the kidneys following FU and/or Cd poisoning could spike their susceptibility to the harmful effects of ROS. Similarly, SOD act as defense against oxidative damage in mitochondria that convert the produced $O_2^{\bullet}$ into O_2 and H2O2 (Abdeen *et al*., 2019b).

Lipid peroxidation has a significant role in the development of renal injury (Ossani *et al*., 2007). Kidney is most vulnerable to harm from ROS. This is most likely due to the high concentration of long-chain polyunsaturated fatty acids (PUFAs) in the lipid composition of the kidneys (Ozbek, 2012). When lipid peroxidation is at a high or moderate level (toxic circumstances), the rate of oxidative damage surpasses the ability for repair. This results in necrosis, apoptosis, or programmed cell death (Ayala *et al*.,

2014). Consistent with the aforementioned assertion, the current study demonstrated a considerable rise in MDA concentrations validating the claim that FU and/or Cd-induced lipid peroxidation leads to damage renal cell membrane this conformed by our histopathological changes that reveal degeneration of renal tubules with vacuolation, hyalinization of renal tubules, necrosis, and dilated tubule. Additionally, both urea and creatinine are sensitive markers to identify renal illnesses and are indicators of kidney impairment (Uthra *et al*., 2017). In our investigation, there were abnormally evoke in level of these parameters in serum when rats were co-exposed to FU and/or Cd. In addition, albumin and total protein levels were considerably lower in of FU and/or Cd group compared to the control group, demonstrating altered renal function. The result of our study are consistent with earlier research that identified elevated blood urea and creatinine levels as indicators of renal impairment brought on by FU (Awad *et al*., 2018; Khalil *et al*., 2020) and Cd treatment (Abdeen *et al*., 2019a; Ijaz *et al*., 2023). These metabolic changes might be a result of tubular damage in renal tissues brought on by FU and/or Cd.

For the evaluation of acute renal failure, KIM-1 is a potential marker. Following exposure to nephrotoxic drugs, proximal tubule cells exhibit increased expression of the type 1 membrane glycoprotein KIM-1. Therefore, elevated levels of this marker indicate kidney damage. This finding supports the theory that Kim-1 is mostly produced in cells that are not fatally wounded as a component of the phagocytic and repair processes that occur in response to injury (Ichimura *et al*., 2008). In our study there were marked increase in the expression profile of Kim-1 when rats were co-exposed to FU and/or Cd exposure in renal tissues compared to control. However, exposure to both toxins manifestly results in an increase in the expression profile of Kim-1 than exposure to either toxin solo. These findings are further supported by the study conducted by Ijaz *et al*. (2023) and Kamel *et al*. (2023) which found that Cd treatment raised the levels of KIM-1, creatinine, and urea in rat kidneys.

Intriguingly, Increased ROS production is expected to initiate an intracellular signaling cascade, increase the expression of proinflammatory genes, and release inflammatory mediators, all of which will lead to a severe inflammatory response (Owumi *et al*., 2020). It also has a significant impact on the activation of inflammatory cytokines such TNF-α, and iNOS. TNF-α is a cytokine that has pleiotropic effects on different kinds of cells. The pathophysiology of some inflammatory and autoimmune illnesses has been linked to it, and it has been recognized as a key regulator of inflammatory responses. It has been functionally demonstrated to initiate a series of different inflammatory chemicals, such as chemokines and other cytokines (Jang *et al*., 2021). Furthermore, nitric oxide produced by iNOS enzymes regulates the inflammatory response. Following the activation of iNOS synthase, NO is produced. This can then combine with the superoxide anion to generate peroxy-nitrite species (ONOO−) (Ben Hsouna *et al*., 2019). Notably, cotreatment with FU and/or Cd exhibited a more noticeable rise in the expression of renal TNF-α and iNOS. These findings are confirmed by previous studies which demonstrate that FU (Owumi *et al*., 2022b) and Cd (Ijaz *et al*., 2023) evoke the expression of renal TNF-α and iNOS.

Members of the water-channel membrane protein family known as AQPs enable water to pass quickly across permeable epithelium, including the kidney tubular epithelium (Kishore *et al*., 2000). Mammals express 13 different AQPs (AQP0–12), each of which has a unique tissue and cellular expression pattern as well as a particular subcellular location. Throughout the renal proximal tubules, Aqp1 is widely distributed throughout the basolateral and apical membranes (Kim *et al*., 2011). It efficiently inhibits the passage of cations, including surplus protons, preserving the osmotic pressure and cytosolic pH of the cell membrane (Li *et al*., 2011). Moreover, Aqp2 a water channel protein transported to renal collecting duct cells, is known to be expressed at a level that regulates renal water excretion (Abdeen *et al*., 2014). The effect of FU and Cd exposure on renal gene expression is scarcely reported. In the meantime, there was a notable down-regulation of the expression of Aqp1 and Aqp2 genes when rats were co-exposed to FU and/or Cd in renal tissues compared to control. However, exposure to both toxins manifestly results in an increase in the expression profile of Aqp1and Aqp2 than exposure to either one alone. Consequently, Kidney damage linked to oxidative stress and renal tubular degeneration may be the cause of the change in the expression profile in the markers under investigation (Mouro *et al*., 2021).

Through both mitochondrial-dependent and -independent mechanisms, an imbalance between apoptotic and antiapoptotic proteins causes apoptosis (Sinha *et al*., 2013). According to our research, apoptotic cell death is a key factor in the pathophysiology of FU and/or Cd -induced nephrotoxicity, which causes damage to kidney cells and a subsequent reduction in kidney function elucidated by increased expression of PCNA after FU and/or Cd exposure in renal tissues of rats. PCNA is thought to be an efficient indicator for cellular proliferation that controls the rates of replicated DNA and the cell cycle. These results corroborate those of Awad *et al*. (2018), who showed increased PCNA immunostaining in rat hepatic tissues following FU exposure, as well as of a different study by Koyuturk *et al*. (2007), which showed that Cd significantly increased PCNA protein expression in hepatic tissues of rat.

Conclusion

Overall, FU or Cd provoked severe nephrotoxicity. Both exposures evoked perturbation in renal function, oxidative stress, together with elevated expression of inflammatory markers as well as apoptotic proteins. Obvious histopathological alteration in the renal tissue was also noticed. Renal damage further confirmed by notable down-regulation of the Aqp1 and Aqp2 genes. Intriguingly, the concurrent FU and Cd intoxication elicited additional extensive renal injury than their individual exposure via triggering oxidative cascade, inflammatory reaction, AQPs downregulation and apoptotic cell death which are thought to be the main mechanisms attributed to this potentiated toxicity.

Acknowledgments

The authors deeply thank the Center of Excellence in Screening of Environmental Contaminants (CESEC), Department of Forensic Medicine and Toxicology, Benha University, Egypt for all the facilities provided for implementing this work.

Conflict of interest

The authors declare that they have no conflict of interest.

References

Abdeen, A., Abou-Zaid, O.A., Abdel-Maksoud, H.A., Aboubakr, M., Abdelkader, A., Abdelnaby, A., Abo-Ahmed, A.I., El-Mleeh, A., Mostafa, O., Abdel-Daim, M., Aleya, L., 2019a, Cadmium overload modulates piroxicam-regulated oxidative damage and apoptotic pathways. Environ. Sci. Pollut. Res. 26, 25167–25177.

Abdeen, A., Aboubakr, M., Elgazzar, D., Abdo, M., Abdelkader, A., Ibrahim, S., Elkomy, A., 2019b, Rosuvastatin attenuates piroxicam-mediated gastric ulceration and hepato-renal toxicity in rats. Biomed. Pharmacother. 110, 895–905.

Abdeen, A., Sonoda, H., El-Shawarby, R., Takahashi, S., Ikeda, M., 2014, Urinary excretion pattern of exosomal aquaporin-2 in rats that received gentamicin. Am. J. Physiol. - Ren. Physiol. 307, 1227–1237.

Abdel-Daim, M.M., Abdeen, A., Jalouli, M., Abdelkader, A., Megahed, A., Alkahtane, A., Almeer, R., Alhoshani, N.M., Al-Johani, N.S., Alkahtani, S., 2021, Fucoidan supplementation modulates hepato-renal oxidative stress and DNA damage induced by aflatoxin B1 intoxication in rats. Sci. Total Environ. 768, 1-13.

Alizadeh, M., Barati, M., Saleh-Ghadimi, S., Roshanravan, N., Zeinalian, R., Jabbari, M., 2018, Industrial furan and its biological effects on the body systems. J. Food Biochem. 42, 1–13.

Almeer, R.S., Soliman, D., Kassab, R.B., AlBasher, G.I., Alarifi, S., Alkahtani, S., Ali, D., Metwally, D., Abdel Moneim, A.E., 2018, Royal jelly abrogates cadmium-induced oxidative challenge in mouse testes: involvement of the Nrf2 pathway. Int. J. Mol. Sci. 19, 3979.

Ansari, M.A., Raish, M., Ahmad, A., Alkharfy, K.M., Ahmad, S.F., Attia, S.M., Alsaad, A.M.S., Bakheet, S.A., 2017, Sinapic acid ameliorate cadmium-induced nephrotoxicity: In vivo possible involvement of oxidative stress, apoptosis, and inflammation via NF-κB downregulation. Environ. Toxicol. Pharmacol. 51, 100–107.

Awad, A., Khalil, S.R., Farag, M.R., Nassan, M.A., 2018, Differential susceptibility of kidneys and livers to proliferative processes and transcriptional level of the genes encoding desmin, vimentin, connexin 43, and nestin in rats exposed to furan. Ecotoxicol. Environ. Saf. 162, 235–244.

Ayala, A., Muñoz, M.F., Argüelles, S., 2014, Lipid peroxidation: production, metabolism, and signaling mechanisms of malondialdehyde and 4-hydroxy-2-nonenal. Oxid. Med. Cell. Longev. 2014,1-31.

Batool, Z., Xu, D., Zhang, X., Li, X., Li, Y., Chen, Z., Li, B., Li, L., 2021, A review on furan: Formation, analysis, occurrence, carcinogenicity, genotoxicity and reduction methods. Crit. Rev. Food Sci. Nutr. 61, 395–406.

Ben Hsouna, A., Gargouri, M., Dhifi, W., Ben Saad, R., Sayahi, N., Mnif, W., Saibi, W., 2019, Potential anti-inflammatory and antioxidant effects of Citrus aurantium essential oil against carbon tetrachloride-mediated hepatotoxicity: A biochemical, molecular and histopathological changes in adult rats. Environ. Toxicol. 34, 388–400.

Brzóska, M.M., Rogalska, J., Galazyn-Sidorczuk, M., Jurczuk, M., Roszczenko, A., Tomczyk, M., 2015, Protective effect of Aronia melanocarpa polyphenols against cadmium-induced disorders in bone metabolism: A study in a rat model of lifetime human exposure to this heavy metal. Chem. Biol. Interact. 229, 132–146.

Cabral, M., Garçon, G., Touré, A., Bah, F., Dewaele, D., Bouhsina, S., Cazier, F., Faye, A., Fall, M., Courcot, D., 2021, Renal impairment assessment on adults living nearby a landfill: Early kidney dysfunction biomarkers linked to the environmental exposure to heavy metals. Toxicol. Reports, 8 386–394.

Dong, H., Gill, S., Curran, I.H., Williams, A., Kuo, B., Wade, M.G., Yauk, C.L., 2016, Toxicogenomic assessment of liver responses following subchronic exposure to furan in Fischer F344 rats. Arch. Toxicol. 90, 1351–1367.

Filipič, M., 2012. Mechanisms of cadmium induced genomic instability. Mutat. Res. Mol. Mech. Mutagen. 733, 69–77.

IARC, 2012, Arsenic, metals, fibres and dusts. IARC Monogr. Eval. Carcinog. risks to humans.100.

Ichimura, T., Asseldonk, E.Jp., Humphreys, B.D., Gunaratnam, L., Duffield, J.S., Bonventre, J. V, 2008, Kidney injury molecule–1 is a phosphatidylserine receptor that confers a phagocytic phenotype on epithelial cells. J. Clin. Invest. 118, 1657–1668.

Ijaz, M.U., Shahzadi, S., Hamza, A., Azmat, R., Anwar, H., Afsar, T., Shafique, H., Bhat, M.A., Naglah, A.M., Al-Omar, M.A., Razak, S., 2023, Alleviative effects of pinostrobin against cadmium-induced renal toxicity in rats by reducing oxidative stress, apoptosis, inflammation, and mitochondrial dysfunction. Front. Nutr. 10, 1-11.

Jang, D.I., Lee, A.H., Shin, H.Y., Song, H.R., Park, J.H., Kang, T.B., Lee, S.R., Yang, S.H., 2021, The role of tumor necrosis factor alpha (Tnf-α) in autoimmune disease and current tnf-α inhibitors in therapeutics. Int. J. Mol. Sci. 22, 1–16.

Kamel, E.O., Gad-Elrab, W.M., Ahmed, M.A., Mohammedsaleh, Z.M., Hassanein, E.H.M., Ali, F.E.M., 2023, Candesartan protects against cadmium-induced hepatorenal syndrome by affecting Nrf2, NF-κB, Bax/Bcl-2/Cyt-C, and Ang II/Ang 1–7 signals. Biol. Trace Elem. Res. 201, 1846–1863.

Khalil, S.R., Salem, H.F.A., Metwally, M.M.M., Emad, R.M., Elbohi, K.M., Ali, S.A., 2020, Protective effect of Spirulina platensis against physiological, ultrastructural and cell proliferation damage

induced by furan in kidney and liver of rat. Ecotoxicol. Environ. Saf. 192, 110256.
Kim, S., Jo, C.H., Park, J.-S., Han, H.J., Kim, G.-H., 2011, The role of proximal nephron in cyclophosphamide-induced water retention: preliminary data. Electrolytes Blood Press. E BP. 9, 7.
Kishore, B.K., Krane, C.M., Di Iulio, D., Menon, A.G., Cacini, W., 2000, Expression of renal aquaporins 1, 2, and 3 in a rat model of cisplatin-induced polyuria. Kidney Int. 58, 701–711.
Klaassen, C.D., Liu, J., Diwan, B.A., 2009, Metallothionein protection of cadmium toxicity. Toxicol. Appl. Pharmacol., 238, 215–220.
Koyuturk, M., Yanardag, R., Bolkent, S., Tunali, S., 2007, The potential role of combined anti-oxidants against cadmium toxicity on liver of rats. Toxicol. Ind. Health 23, 393–401.
Kumar, A., Sharma, B., 2018, Consequences of heavy metals pollution in environment and bioremediation practices. Recent Adv. Environ. Manag. Bharagava, RN, Ed.; CRC Press. Taylor Fr. Gr. Boca Raton, FL, USA., pp. 247–273.
Li, H., Chen, H., Steinbronn, C., Wu, B., Beitz, E., Zeuthen, T., Voth, G.A., 2011, Enhancement of Proton Conductance by Mutations of the Selectivity Filter of Aquaporin-1. J. Mol. Biol. 407, 607–620.
McDaniel, L.P., Ding, W., Dobrovolsky, V.N., Shaddock Jr, J.G., Mittelstaedt, R.A., Doerge, D.R., Heflich, R.H., 2012, Genotoxicity of furan in Big Blue rats. Mutat. Res. Toxicol. Environ. Mutagen. 742, 72–78.
Mouro, V.G.S., Ladeira, L.C.M., Lozi, A.A., de Medeiros, T.S., Silva, M.R., de Oliveira, E.L., de Melo, F.C.S.A., da Matta, S.L.P., 2021, Different routes of administration lead to different oxidative damage and tissue disorganization levels on the subacute cadmium toxicity in the liver. Biol. Trace Elem. Res., 199, 1–11.
Olayan, E.M., Aloufi, A.S., AlAmri, O.D., Ola, H., Moneim, A.E.A., 2020. Protocatechuic acid mitigates cadmium-induced neurotoxicity in rats: Role of oxidative stress, inflammation and apoptosis. Sci. Total Environ. 723, 137969.
Ossani, G., Dalghi, M., Repetto, M., 2007, Oxidative damage lipid peroxidation in the kidney of choline-deficient rats. Front. Biosci. 12, 1174–1183.
Owumi, S.E., Arunsi, U.O., Otunla, M.T., Oluwasuji, I.O., 2022a, Exposure to lead and dietary furan intake aggravates hypothalamus-pituitary-testicular axis toxicity in chronic experimental rats. J. Biomed. Res. 37, 100-114.
Owumi, S.E., Bello, S.A., Idowu, T.B., Arunsi, U.O., Oyelere, A.K., 2022b, Protocatechuic acid protects against hepatorenal toxicities in rats exposed to Furan. Drug Chem. Toxicol. 45, 1840–1850.
Owumi, S.E., Ijadele, A.O., Arunsi, U.O., Odunola, O.A., 2020, Luteolin abates reproductive toxicity mediated by the oxido-inflammatory response in Doxorubicin-treated rats. Toxicol. Res. Appl. 4, 1-16.
Ozbek, E., 2012, Induction of oxidative stress in kidney. Int. J. Nephrol. 2012, 1-2.
Pfaffl, M.W., 2001, A new mathematical model for relative quantification in real-time RT–PCR. Nucleic Acids Res. 29, 1-6.
Phillips, M.B., Sullivan, M.M., Villalta, P.W., Peterson, L.A., 2014, Covalent modification of cytochrome c by reactive metabolites of furan. Chem. Res. Toxicol. 27, 129–135.
Poli, V., Madduru, R., Aparna, Y., Kandukuri, V., Motireddy, S.R., 2022, Amelioration of Cadmium-Induced Oxidative Damage in Wistar Rats by Vitamin C, Zinc and N-Acetylcysteine. Med. Sci. 10, 1-16.
Rahimzadeh, Mehrdad Rafati, Rahimzadeh, Mehravar Rafati, Kazemi, S., Moghadamnia, A., 2017, Cadmium toxicity and treatment: An update. Casp. J. Intern. Med. 8, 135.
Rani, A., Kumar, A., Lal, A., Pant, M., 2014, Cellular mechanisms of cadmium-induced toxicity: A review. Int. J. Environ. Health Res. 24, 378–399.
Samarghandian, S., Azimi-Nezhad, M., Shabestari, M.M., Azad, F.J., Farkhondeh, T., Bafandeh, F., 2015, Effect of chronic exposure to cadmium on serum lipid, lipoprotein and oxidative stress indices in male rats. Interdiscip. Toxicol. 8, 151.
Seif, M.M., Madboli, A.N., Marrez, D.A., Aboulthana, W.M.K., 2019, Hepato-Renal protective Effects of Egyptian Purslane Extract against Experimental Cadmium Toxicity in Rats with Special Emphasis on the Functional and Histopathological Changes. Toxicol. Reports. 6, 625–631.
Seok, Y.-J., Her, J.-Y., Kim, Y.-G., Kim, M.Y., Jeong, S.Y., Kim, M.K., Lee, J., Kim, C., Yoon, H.-J., Lee, K.-G., 2015. Furan in thermally processed foods-a review. Toxicol. Res. 31, 241–253.
Setia, R., Dhaliwal, S.S., Kumar, V., Singh, R., Kukal, S.S., Pateriya, B., 2020, Impact assessment of metal contamination in surface water of Sutlej River (India) on human health risks. Environ. Pollut. 265, 1-32.
Sinha, K., Das, J., Pal, P.B., Sil, P.C., 2013, Oxidative stress: the mitochondria-dependent and mitochondria-independent pathways of apoptosis. Arch. Toxicol. 87, 1157–1180.
Starowicz, M., Ostaszyk, A., Zieliński, H., 2021, The relationship between the browning index, total phenolics, color, and antioxidant activity of polish-originated honey samples. Foods 10, 1-12.
Tăbăran, A.-F., O'Sullivan, M.G., Seabloom, D.E., Vevang, K.R., Smith, W.E., Wiedmann, T.S., Peterson, L.A., 2019, Inhaled furan selectively damages club cells in lungs of A/J mice. Toxicol. Pathol. 47, 842–850.
Uddin, M.J., Kim, E.H., Hannan, M.A., Ha, H., 2021, Pharmacotherapy against oxidative stress in chronic kidney disease: Promising small molecule natural products targeting nrf2-ho-1 signaling. Antioxidants 10, 1-26.
Uthra, C., Shrivastava, S., Jaswal, A., Sinha, N., Reshi, M.S., Shukla, S., 2017, Therapeutic potential of quercetin against acrylamide induced toxicity in rats. Biomed. Pharmacother. 86, 705–714.
Yilmaz, S., Kaya, E., Kisacam, M.A., 2017, The effect on oxidative stress of aflatoxin and protective effect of lycopene on aflatoxin damage. Aflatoxin-control, Anal. Detect. Heal. Risks 30, 67–90.